Simulating the effects of climate and agricultural management practices on global crop yield

D. Deryng,[1,2] W. J. Sacks,[3] C. C. Barford,[3] and N. Ramankutty[1]

Received 20 December 2009; revised 23 November 2010; accepted 25 February 2011; published 20 May 2011.

[1] Climate change is expected to significantly impact global food production, and it is important to understand the potential geographic distribution of yield losses and the means to alleviate them. This study presents a new global crop model, PEGASUS 1.0 (Predicting Ecosystem Goods And Services Using Scenarios) that integrates, in addition to climate, the effect of planting dates and cultivar choices, irrigation, and fertilizer application on crop yield for maize, soybean, and spring wheat. PEGASUS combines carbon dynamics for crops with a surface energy and soil water balance model. It also benefits from the recent development of a suite of global data sets and analyses that serve as model inputs or as calibration data. These include data on crop planting and harvesting dates, crop-specific irrigated areas, a global analysis of yield gaps, and harvested area and yield of major crops. Model results for present-day climate and farm management compare reasonably well with global data. Simulated planting and harvesting dates are within the range of crop calendar observations in more than 75% of the total crop-harvested areas. Correlation of simulated and observed crop yields indicates a weighted coefficient of determination, with the weighting based on crop-harvested area, of 0.81 for maize, 0.66 for soybean, and 0.45 for spring wheat. We found that changes in temperature and precipitation as predicted by global climate models for the 2050s lead to a global yield reduction if planting and harvesting dates remain unchanged. However, adapting planting dates and cultivar choices increases yield in temperate regions and avoids 7–18% of global losses.

Citation: Deryng, D., W. J. Sacks, C. C. Barford, and N. Ramankutty (2011), Simulating the effects of climate and agricultural management practices on global crop yield, *Global Biogeochem. Cycles*, *25*, GB2006, doi:10.1029/2009GB003765.

1. Introduction

[2] Global food production will need to keep increasing in order to meet future demand, which is expected to rise due to economic development and population growth in developing countries [*Von Braun*, 2007]. World population is anticipated to stabilize around 10 billion people by 2100; however, a shift toward more meat consumptive diets in emerging economic countries adds further pressure on global cereal supplies [*Keyzer et al.*, 2002; *Lutz et al.*, 2001]. In addition, the growing interest in biofuels contributes to increased demand for the production of crops like soybean and maize [*Von Braun*, 2007].

[3] During the past 50 years, technological progress in farm management contributed to a large increase in global crop yield, which enabled production to satisfy demand on a global average. While global harvested area remained steady, global crop production expanded considerably as a result of large increases in chemical fertilizer and pesticide use, expansion of irrigated areas, and development of high yielding crop varieties [*Cassman*, 1999; *Food and Agriculture Organization* (*FAO*), 2009; *Tilman et al.*, 2001].

[4] Nevertheless, challenges remain for the future. First of all, it is uncertain whether more productive cultivars can continuously be developed in the future [*Tilman et al.*, 2002]. Second, energy resources to produce fertilizer, as well as land and water resources, are limited and might limit future agricultural production [*Foley et al.*, 2007; *Harris and Kennedy*, 1999; *Lotze-Campen et al.*, 2008; *Postel*, 1998]. Finally, climate change represents a major concern for future food production, particularly in developing regions where more frequent droughts and floods are anticipated [*Lobell et al.*, 2008; *Nelson et al.*, 2009; *Parry et al.*, 2005; *Rosenzweig and Parry*, 1994; *Von Braun*, 2007].

[5] Identifying the best adaptation strategies for farming is necessary in order to mitigate risks induced by climate change. Indeed, with a changing climate, farmers will have to adapt current production practices to cope with more frequent climate hazards and to new climate trends. These adaptations include changing crop varieties in order to take

[1]Department of Geography, McGill University, Montreal, Quebec, Canada.
[2]Tyndall Centre, School of Environmental Sciences, University of East Anglia, Norwich, UK.
[3]Center for Sustainability and the Global Environment, University of Wisconsin-Madison, Madison, Wisconsin, USA.

0886-6236/11/2009GB003765

advantage of a longer growing season in high latitudes, shifting sowing dates, and adjusting various water, fertilizer, and pest management options [*Howden et al.*, 2007]. As an example, *Kucharik* [2008] showed that maize yield in some states of the United States increased by more than 20% in the last 25 years on account of earlier planting and other associated management changes.

[6] To date, a few global studies have attempted to assess the future of world food production in the context of climate change. Various modeling techniques have been used from detailed process-based models to more general statistical analyses and empirical models. *Leemans and Solomon* [1993] combined a simple water balance model with the Agro-Ecological Zones (AEZ) methodology [*FAO*, 1978] to quantify the potential effect of climate change on rain-fed crop yield and its geographic distribution. *Fischer et al.* [2002a] further expanded this empirical approach with the Global Agro-Ecological Zones (GAEZ), which includes more recent data on land resources and irrigated agriculture.

[7] Statistical models have been developed by analyzing historical relationships between climate and crop yield [*Lobell and Asner*, 2003; *Lobell and Field*, 2007; *Lobell et al.*, 2008; *Schlenker and Roberts*, 2009]. While this method is easily applicable at the global scale, uncertainties remain large due to inherent errors from the input data sets. Furthermore, these studies do not include a process-based understanding of the system, and therefore make a major assumption that present-day statistical relationships between crop yields and climate will hold true in the future.

[8] *Rosenzweig and Parry* [1994], and then *Parry et al.* [1999, 2005], used a set of detailed process-based models to evaluate global consequences of various climate change scenarios on world food production. These models include detailed crop management options and crop physiology characteristics, but necessitate substantial amounts of data to calibrate the model to a particular location. Consequently, these models were applied to a limited number of sites around the world and the results were aggregated in order to present general conclusions at the global scale.

[9] Using a more complex process-based methodology, Agro-IBIS [*Kucharik and Brye*, 2003], and ORCHIDEE-STICS [*Gervois et al.*, 2004; *de Noblet-Ducoudré et al.*, 2004] successfully implemented detailed crop modeling frameworks into global vegetation models. These models were applied in large-scale analyses over the United States using Agro-IBIS [*Kucharik and Brye*, 2003] and over western Europe using ORCHIDEE-STICS [*Gervois et al.*, 2008], but have not been expanded to the global scale. The complexity of the model (Agro-IBIS) or the lack of global data (ORCHIDEE-STICS) make it difficult to apply these models at the global scale.

[10] Only recently have global ecosystem models begun to consider agroecosystems [*Scholze et al.*, 2005]. Lately, three global-scale crop models have been published. First, *Osborne et al.* [2007] focus mainly on the interaction between crop and climate by integrating the crop model GLAM into the land surface component of a global climate model; it does not explicitly include detailed agricultural management practices. Second, the Lund-Potsdam-Jena managed Land (LPJmL) model [*Bondeau et al.*, 2007] extends the LPJ-Dynamic global vegetation model that simulates biophysical and biogeochemical processes associated with global carbon and water cycles. This model uses a crop functional type (CFT) strategy in order to simulate yields of the 13 most important crop types in the world. Third, the DayCent model, which was primarily developed to study the biogeochemical cycling of nutrients in agroecosystems, simulates global crop production of four leading crops: wheat, maize, rice, and soybean [*Stehfest et al.*, 2007]. Both LPJmL and DayCent carefully represent biophysical and biogeochemical processes, and include a few farm management practices. LPJmL explicitly simulates planting decisions for some CFTs, and DayCent calculates optimum planting dates according to climate. In addition, both models include the effect of irrigation and fertilizer application. DayCent explicitly simulates nutrient cycling to represent the effect of nitrogen fertilizer and manure application, while LPJmL scales maximum leaf area index depending on fertilizer application, but only for two CFTs. Nevertheless, representation of planting/harvesting dates, fertilizer application; this was likely due to the lack of accurate and spatially explicit input data available at the time of development of those models.

[11] The purpose of this paper is to present a new global crop yield model, PEGASUS 1.0 (Predicting Ecosystem Goods And Services Using Scenarios) that explicitly simulates crop phenology and the influence of irrigation and fertilizer use. This new model benefits from the recent development of a suite of global data sets that form valuable model inputs or are suitable for model calibration. In particular, we use new global data sets of crop planting and harvesting dates [*Sacks et al.*, 2010], annual harvested areas of irrigated crops [*Portmann et al.*, 2010], national data on chemical fertilizer application rate by crop [*International Fertilizer Industry Association (IFA)*, 2002], the global distribution of crop-harvested areas and yields [*Monfreda et al.*, 2008], and a recent analysis of the global distribution of yield gaps [*Licker et al.*, 2010]. We developed algorithms to simulate planting and cultivar choice decisions as functions of simple climate variables. Thus, PEGASUS has the ability to simulate the effect of climate change on planting decisions and implicitly represents crop cultivar choices at the global scale. In addition, PEGASUS is capable of simulating the impact of future scenarios of irrigation and chemical fertilizer use on crop yields. PEGASUS is calibrated against a recently developed global data set of crop yields [*Monfreda et al.*, 2008].

[12] This paper presents a detailed description of the model in section 2, the calibration method in section 3, and the model evaluation against present-day data in section 4. Finally, a simple climate sensitivity analysis illustrates the effect of changes in temperature and precipitation on global crop yields in section 5.

2. Model Description

[13] PEGASUS combines a light use efficiency (LUE) model to estimate daily photosynthesis and annual net primary production (NPP) [*Haxeltine and Prentice*, 1996] with a surface energy and soil water budget model [*Foley*, 1994; *Gerten et al.*, 2004; *Ramankutty et al.*, 2002]. In addition, the model uses a dynamic allocation scheme to assign daily biomass production to the different organs of the crop [*Penning de Vries et al.*, 1989]. Thus, crop yield is

eventually derived from the amount of carbon contained in the storage organs at harvesting date. In this study, we focus on three crops: maize, soybeans, and spring wheat.

[14] The model is driven by daily climate data of temperature, precipitation, and potential sunshine hours. Daily data come from linear interpolation of the CRU monthly climatology of the global land surface at 10′ latitude/longitude resolution, developed by *New et al.* [2002]. In addition to climate data, the model uses ISRIC-WISE soil data on available water capacity [*Batjes*, 2006]. Finally, simulations for present-day crop yield use the MIRCA2000 data set on global irrigated cropland area [*Portmann et al.*, 2010] and the IFA data on national rate of fertilizer application [*IFA*, 2002]. These fertilizer data exclude countries that do not apply much fertilizer. Hence, we assumed that countries without fertilizer data have a fertilizer application rate of zero. This study also uses the M3 crops data [*Monfreda et al.*, 2008]. Soil, irrigation, crop yield and crop-harvested area were all originally developed at 5′ latitude × 5′ longitude resolution. We therefore aggregated these data to 10′ latitude × 10′ longitude resolution in order to match the input climate data. Fertilizer data consist of national averages, thus one unique value was used for all cultivated pixels within each nation. Table 1 describes the specific data sets used in this study.

2.1. Daily Biomass Production

[15] The LUE model assumes photosynthesis in unstressed conditions is proportional to incoming solar radiation. Additionally, temperature, soil moisture availability, and nutrient availability can limit daily net biomass production ($\mathcal{P}$). $\mathcal{P}$ is expressed in mol C m^{-2} s^{-1} as

$$\mathcal{P} = \varepsilon \mathrm{APAR} f_T f_W f_N \tag{1}$$

where ε (mol C mol $quanta^{-1}$) is the light use efficiency coefficient. We tuned this parameter by calibrating PEGASUS-simulated yield to actual crop yield data (section 3). APAR (mol quanta m^{-2} s^{-1}) represents the daily average absorbed photosynthetically active radiation and is expressed using Beer-Lambert's law for light interception on a surface [*Foley*, 1994], which is a function of the crop leaf area index (LAI):

$$\mathrm{LAI} = C_l \times \mathrm{SLA} \tag{2}$$

where C_l is the carbon content in leaves (kg C m^{-2}), and SLA (m^2 kg C^{-1}) is the specific leaf area (Table 2). f_T, f_W, and f_N are three limiting factors varying between 0 (high stress) and 1 (no stress) of daily mean temperature, daily soil moisture, and soil nutrient status, respectively.

[16] Other limiting factors such as pests and diseases, air pollution, soil erosion, level of mechanization and farmer-style of management are not taken into consideration. This simple global crop model is based on three major assumptions. First, we assume soil nutrient content has a predominant effect on crop yield relatively to these other limiting factors. Second, as no crop specific data on manure application exists at the global scale, we assume chemical fertilizer inputs dominate over manure application. As a result, the nutrient stress factor (f_N) depends solely on chemical fertilizer application. Third, we assume a positive correlation between the rate of chemical fertilizer application and other limiting factors; that is, places with high rate of chemical fertilizer applications should have higher level of mechanization and higher use of chemical pesticides. Thus, f_N encompasses a variety of farm management practices, mainly driven by chemical fertilizer application (see section 2.4). Although irrigation intensity is also linked to the level of mechanization, we use an independent water stress factor (f_W) as the availability of crop specific spatial data on irrigated cropland areas are available, whereas global data on the rate of chemical fertilizer application for specific crops exist only as national averages.

2.2. Temperature Limitation

[17] The temperature stress factor (f_T) is defined separately for each crop type according to the crop's temperature requirements [*Kucharik and Brye*, 2003] (Figure 1a). Site-specific crop models usually apply a function with a narrow temperature range adapted to each crop cultivar [*Sharpley and Williams*, 1990]. Indeed, optimum and extreme temperature requirements of a specific crop vary across the world since farmers tend to select cultivars to maximize yield according to local climate conditions [*Penning de Vries et al.*, 1989]. However, PEGASUS uses a stress function with a wider temperature range where yields are optimum in order to reproduce global patterns better (i.e., our stress function is an envelope of the individual stress functions of each cultivar).

2.3. Water Limitation and Irrigation

[18] The water stress factor (f_W) is a function of the potential plant water uptake rate U_p [*Campbell and Norman*, 2000], which is a nonlinear function of the ratio of the soil water SW to the soil available water capacity (AWC) (Figure 1b). Potential plant water uptake is high as long as soil water exceeds half of the soil available water capacity, but it decreases rapidly below this threshold. The calculation of daily soil moisture follows a simple two-layer bucket approach, driven by the Priestley-Taylor equation to estimate potential evapotranspiration (PET). A more detailed description of the surface energy and water budget calculation is given by *Gerten et al.* [2004]; *Ramankutty et al.* [2002].

[19] We used global maps of crop-specific irrigated area from the global data set of Monthly Irrigated and Rainfed Crop Areas around the year 2000 (MIRCA2000 [*Portmann et al.*, 2010]). We estimated the fraction of irrigated versus rain-fed crop areas using global maps of crop-specific harvested area [*Monfreda et al.*, 2008], and we ensured that soil is sufficiently moist to avoid water stress in irrigated land (Figure 1b). Thus, the resulting water stress function of a given pixel (f_W) is a linear combination of potential water uptake rate in irrigated and rain-fed condition:

$$f_W = \frac{A_i}{A_h}\max\left(0.9, U_p\right) + \left(1 - \frac{A_i}{A_h}\right)U_p \tag{3}$$

where A_i and A_h correspond to crop-irrigated area and harvested area, respectively, and U_p is the potential plant water uptake rate shown in Figure 1b.

Table 1. Minimum Data Requirements to Run PEGASUS and Description of the Specific Data Sets Used in This Study

Data Set	Variable Name	Spatial Reference	Temporal Reference	Source
Climate data (CRU)	temperature, precipitation, fraction of sunshine hours	10′ lat × 10′ lon	monthly average 1961–1990	*New et al.* [2002]
Soil data (ISRIC-WISE)	Available water capacity (top 50 cm, top 20 cm, 50–150 cm soil columns)	10′ lat × 10′ lon (original is 5′ lat × 5′ lon)	-	*Batjes* [2006]
Irrigation data (MIRCA 2000)	Annual irrigated harvested area	10′ lat × 10′ lon (original is 5′ lat × 5′ lon)	2000	*Portmann et al.* [2010]
Fertilizer data	total chemical fertilizer application	national average	mid-1990s	*IFA* [2002]
M3-crops data	Yield, Harvested area	′ lat × 10′ lon (original is 5′ lat × 5′ lon)	average for 1998–2002	*Monfreda et al.* [2008]
Global crop calendar	planting dates, harvesting dates	10′ lat × 10′ lon	1990s and early 2000s	*Sacks et al.* [2010]

[20] Another way to simulate both irrigated and rain-fed production consists of simulating irrigated and rain-fed systems separately and then combining the resulting yields using the map of irrigated areas. However, we found that using this alternative method did not change the results much. Thus, we used the linear combination of potential water uptake rates to simplify the computations. Soil water is computed daily assuming daily water application in irrigated land as necessary to avoid water stress. However, irrigation in PEGASUS does not take into account differences in irrigation efficiency due to different types of irrigation infrastructure.

2.4. Nutrient Limitation and Fertilizer Application

[21] The nutrient stress factor (f_N) was determined after analyzing the correlation between national rates of chemical fertilizer application (nitrogen, phosphorus and potassium) from *IFA* [2002] and yield gap fraction data at 10′ latitude × 10′ longitude resolution from *Licker et al.* [2010].

[22] *Licker et al.* [2010] performed a spatial analysis of potential yield achievable according to specific soil moisture and temperature conditions for 18 crops in the world. They defined 100 climate zones and estimated potential yield by selecting the 90th percentile yield from distributions of yields within each climate zone. They then created maps of potential yield based on knowledge of the climate zone each pixel belonged to and they used the spatial data on actual yield to estimate yield gap spatially, so that

$$f_{\text{Yield Gap}} \equiv 1 - \frac{Y_{\text{actual}}}{Y_{\text{potential}}} \tag{4}$$

where $f_{\text{Yield Gap}}$ is the yield gap fraction, Y_{actual} is the actual yield, and $Y_{\text{potential}}$ is the potential yield. *Licker et al.* [2010] attributed the yield gap to a combination of management factors. The most important of these are probably irrigation and fertilization. We assumed that, in irrigated croplands, the yield gap could be attributed entirely to nutrient limitation, so

$$f_{\text{Yield Gap,irr}} = 1 - \frac{Y_{\text{actual}}}{Y_{N_{\text{opt}}}} \tag{5}$$

where $Y_{N\text{opt}}$ is the yield achievable without nutrient limitation. We further assumed that the yield gap could be expressed equivalently in terms of a ratio of daily biomass production rates rather than a ratio of yields

$$f_{\text{Yield Gap,irr}} = 1 - \frac{\mathcal{P}}{\mathcal{P}_{N_{opt}}} = 1 - f_N \tag{6}$$

where $\mathcal{P}_{N\text{opt}}$ is the daily biomass production rate with no nutrient limitation (i.e., $f_N = 1$), but with the same values of ε, APAR, f_T and f_W as for $\mathcal{P}$.

Table 2. Crop Parameters and Values[a]

	Maize	Spring wheat	Soybean
Albedo	0.20	0.21	0.23
Specific leaf area SLA (m^2 kg C^{-1})	50	45	56
Light use efficiency ε (mol C m^{-2} s^{-1} APAR)	0.033	0.027	0.010
Economic fraction EF	0.70	0.85	0.70
Dry fraction DF	0.89	0.89	0.90
Nutrients stress factor f_N	$f_N = 1 - (0.4574–0.0010 \times \mathcal{F})$	$f_N = 1 - (0.4782–0.0015 \times \mathcal{F})$	$f_N = 1$
Temperature at planting in temperature-limited regions (°C)	No snow: $T_{plant} = -5.3 + 1.5T_{amean}$ Snow: $T_{plant} = 16$°C	$T_{plant} = 10$°C	$T_{plant} = 9 + 0.9T_{amean}$
P/PET at planting in moisture-limited regions	P/PET = 0.6	P/PET = 0.7	P/PET = 1.2
Planting date in non-climate-limited regions	DOY_{plant} = 130 (NH)/320 (SH)	DOY_{plant} = 70 (NH)/180 (SH)	DOY_{plant} = 70 (NH)/320 (SH)
Base temperature T_b (°C)	8	0	10
Maximum temperature $T_{\max}$ (°C)	30	26	30
Total GDD requirements (°Cday)	$2033 \times (1 - e^{-\text{aGDD}/1295})$	$2023 \times (1 - e^{-\text{aGDD}/2630})$	$2728 \times (1 - e^{-\text{aGDD}/2295})$
Minimum GDD threshold (°Cday)	683	1449	975
Fraction of total GDD to emerge	0.03	0.03	0.05

[a] $\mathcal{F}$ is the rate of fertilizer application (kg Ha^{-1}), T_{amean} is the annual mean temperature, T_{plant} is the temperature at planting, P/PET is the ratio of precipitation to potential evapotranspiration, DOY_{plant} is the planting date, GDD stands for growing degree day, and aGDD is the annual growing degree day. NH and SH correspond to Northern and Southern Hemispheres, respectively.

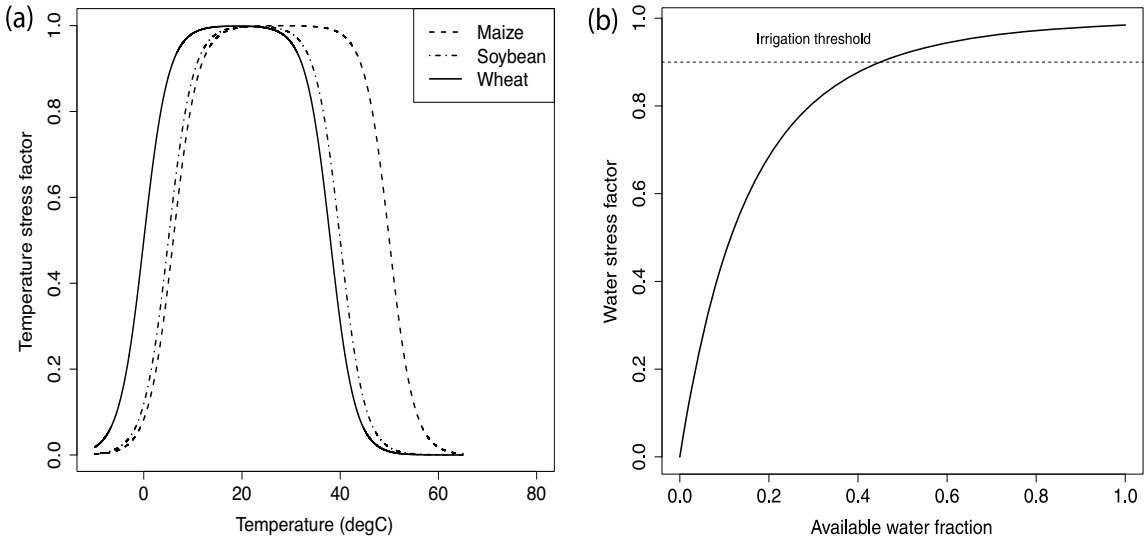

Figure 1. (a) Temperature-stress factors associated with each crop type [*Kucharik and Brye*, 2003]. (b) Potential plant water uptake index expressed as a function of the soil available water fraction (ratio of soil available water to field capacity) [*Campbell and Norman*, 2000]. In irrigated cropland, the potential water uptake index is always above 0.9.

[23] Finally, we assumed that f_N is proportional to the fertilizer application rate ($\mathcal{F}$), so that

$$f_{\text{Yield Gap,irr}} = 1 - f_N = a - b \times \mathcal{F} \tag{7}$$

We then estimated the coefficients a and b by performing a linear regression of $f_{\text{Yield Gap,irr}}$ on $\mathcal{F}$, and derived an expression for f_N as a function of $\mathcal{F}$ from equation (7). In order to estimate f_N, we selected "irrigated" pixels as those with more than 20% of the cropland area under irrigation, assuming negligible water stress in these places, i.e., the yield gap being mainly driven by nutrient limitation. Note that we choose this particular threshold in order to have enough data points to perform the regression analysis. As only national average data of chemical fertilizer application are available, we calculated weighted national average yield gap fractions for these irrigated pixels in each country, with the weighting based on crop-irrigated areas given by the MIRCA2000 data set [*Portmann et al.*, 2010]. Figure 2 shows the resulting linear regressions between national yield gap fraction and the rate of chemical fertilizer application. The functional forms for f_N are given in Table 2.

[24] While the analysis for maize and spring wheat revealed statistical relationships, the analysis for soybean did not display any relationship. Soybean differs from maize and spring wheat as it fixes nitrogen directly from the atmosphere, thereby not requiring substantial nitrogen input to the soil [*Salvagiotti et al.*, 2008]. Nevertheless, it still needs adequate soil concentrations of phosphorus and potassium. Even when our analysis considered all three chemicals, no relationship emerged given the small number of countries growing fertilized soybean in more than 20% irrigated cropland areas. Another major issue arising from the absence of a nutrient stress factor for soybean simulations is related to our assumption that f_N comprises indirectly the effect of a number of other management practices (section 2.1). Future efforts to improve PEGASUS will need to consider more carefully the role of those various management practices on soybean yield.

2.5. Planting and Cultivar Choice Decisions

[25] Planting and harvesting dates are necessary inputs to the crop model. We investigated the relationship between crop calendars and climate data in order to simulate planting and harvesting dates (the difference between the two reflecting cultivar choice) according to simple climatic variables. *Sacks et al.* [2010] recently developed a global crop calendar data set consisting of both the mean and a range of planting and harvesting dates at national and subnational levels compiled from the U.S. Department of Agriculture (USDA) and FAO. We used the mean dates to perform this analysis and computed weighted averages of climate and any other relevant variables for each of the political regions, with the weighting based on global maps of crop-harvested areas from *Monfreda et al.* [2008]. Table 2 presents a summary of the algorithm for planting and harvesting decisions for the three crops.

2.5.1. Planting Dates

[26] Although planting decisions may also be influenced by other factors such as labor and tractor availability, we assume that climate is generally a strong determinant of planting dates in many regions. For instance, in temperate regions, planting occurs when temperature is at least sufficiently warm to protect crops from frost. Similarly, in tropical regions with distinct wet and dry periods, planting usually occurs at the start of the rainy season [*Sacks et al.*,

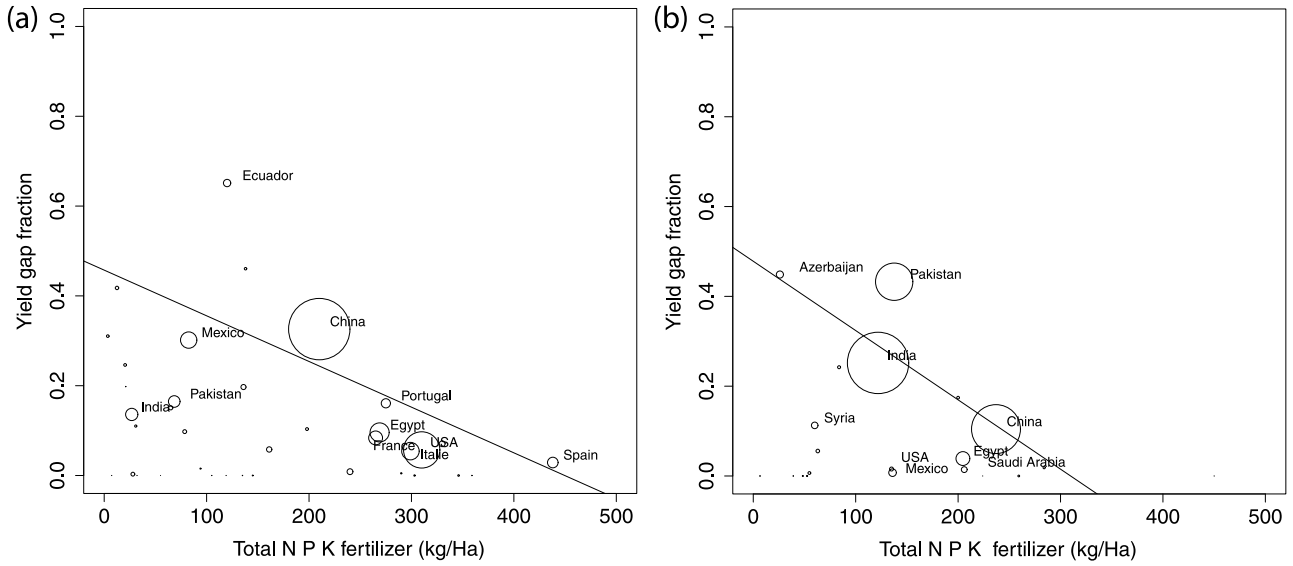

Figure 2. Scatterplots of national average yield gap fractions in irrigated areas versus total chemical fertilizer application. We calculated weighted average yield gap fractions by selecting only pixels where more than 20% of the crop-harvested area is irrigated, using global maps of yield gap fraction [*Licker et al.*, 2010], irrigated areas [*Portmann et al.*, 2010], and harvested area [*Monfreda et al.*, 2008] for each crop. The spatial weighting to derive the national averages was based on crop-irrigated areas. We used national rate of total chemical fertilizer application from *IFA* [2002]. Areas of circles represent crop-irrigated area. Note that the yield gap fraction reaches a maximum threshold when total fertilizer application equals zero, so that f_N is always greater than a minimum threshold.

2010]. Therefore, we distinguish two main climate-limited regions: temperature-limited regions and non–temperature-limited but soil moisture-limited regions (hereafter referred to as moisture-limited regions for simplicity). We hypothesize that temperature is the strongest determinant of planting decision in temperature-limited regions, while soil moisture is more influential in moisture-limited regions.

[27] Following *Leemans and Solomon* [1993] and the GAEZ methodology [*Fischer et al.*, 2002b], the growing period of a crop is based on temperature, precipitation, and potential evapotranspiration (PET). By this definition, a region is temperature-limited if the minimum monthly mean temperature is less than 5 for at least one month. Similarly, a region is moisture-limited if daily precipitation falls below half of PET for more than 30 days in the year. Note that these simple criteria are based on empirical findings of what monthly mean temperature or rainfall has to be in order for a place to temperature or moisture limited. Finally, for non–climate-limited regions, we assumed that planting occurs on one predominant day independent of climate, although this day varies by crop and hemisphere.

[28] We assumed planting date is mainly determined by temperature in temperature-limited regions. However, temperature at planting is likely not uniform globally; instead, it is likely that warmer regions can afford to wait a little longer and plant at warmer temperatures, while colder regions will plant earlier at colder temperatures. We empirically identified this relationship between temperature at planting and annual mean temperature through a regression analysis (Figure 3). Whenever the coefficient of determination (R^2) was lower than 0.6, we simply used the modal value of temperature at planting, using a bin size of 1. We also considered the influence of winter snow on planting dates. Snow accumulation can delay planting since farmers have to wait until the soil is dry enough to drive tractors in the fields. We analyzed patterns of temperature at planting in regions where annual snowpack is greater than zero, separately from other temperature-limited regions. However, empirically, we were able to make this distinction only for maize, which is an important crop in both regions with and without winter snow. In temperature-limited regions, soybean is mainly grown in places that do not experience winter snow, while spring wheat is mostly grown in places with winter snow, providing few samples for a robust statistical analysis. In moisture-limited regions, we determined the appropriate planting time by selecting the modal value of the ratio of precipitation to PET at planting, using a bin size of 0.1(Figure 3). Finally, in non–climate-limited regions, we chose the modal value of planting date by considering histograms of planting dates, using a bin size of 1 day (figure not shown).

2.5.2. Harvest Dates

[29] The length of the growing period of a crop depends on the thermal time accumulation, which is also designated as growing degree days (GDD). Crop models traditionally use GDD accumulation in order to predict harvesting dates: each crop needs a specific GDD amount to reach physiological maturity, and harvest occurs when this requirement is met. The equation to calculate total GDD is

$$\mathrm{GDD}_{T_b} = \sum_{i=1}^{N} \max(0, \min(T_i, T_{\max}) - T_b) \tag{8}$$

where T_i is the daily mean temperature at day i, T_b is the base temperature, $T_{\max}$ is the maximum temperature

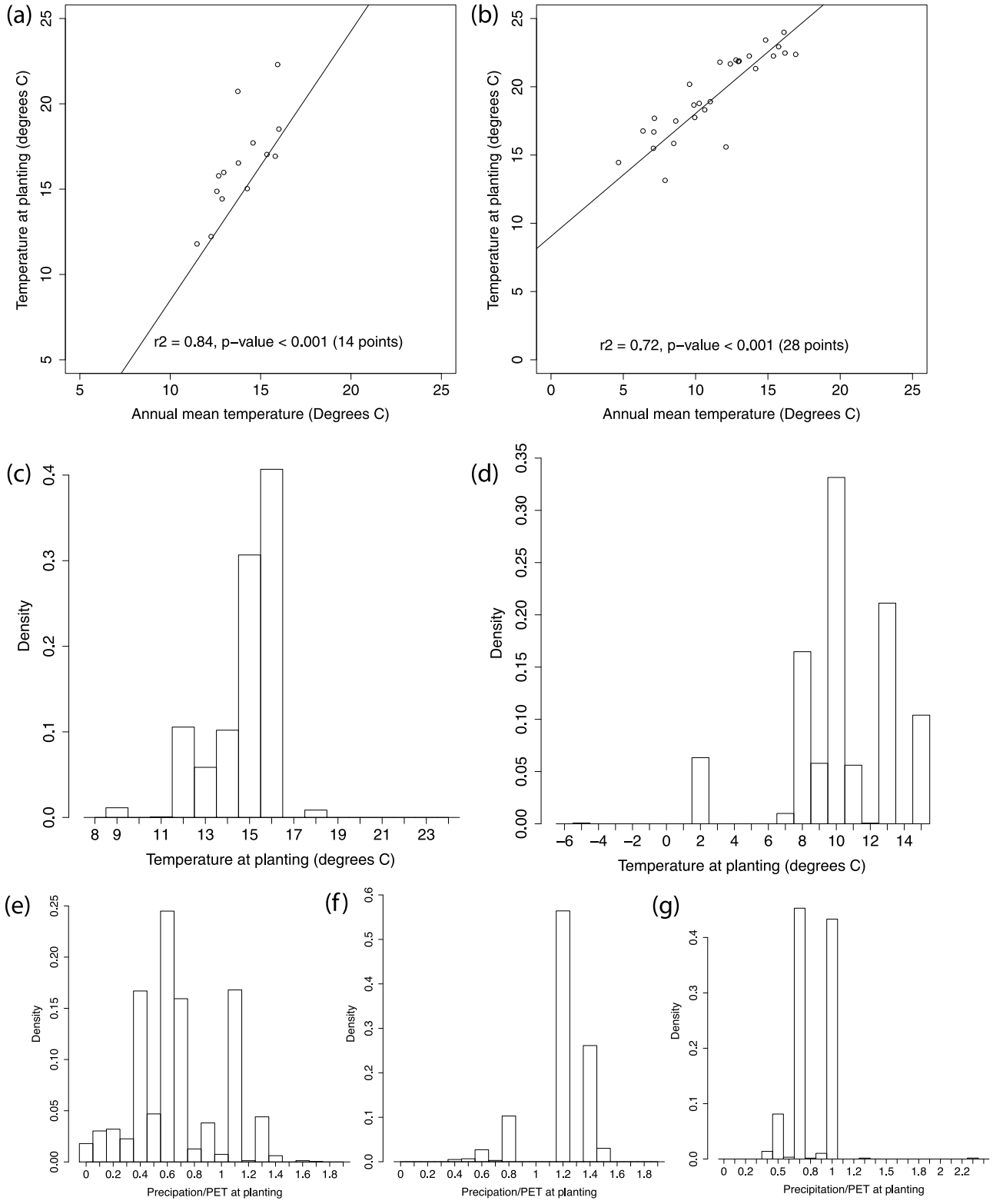

Figure 3. Scatterplots of average temperature at planting versus annual mean temperature in temperature-limited regions (a) for maize (regions without winter snow only) and (b) for soybean. Distributions of the average temperature at planting in temperature-limited regions (c) for maize (regions with winter snow only) and (d) for spring wheat. Distributions of the average precipitation/PET at planting in moisture-limited regions for (e) maize, (f) soybean, and (g) spring wheat. We calculated weighted average climate values in each region, with the weighting based on the total crop-harvested area in that region.

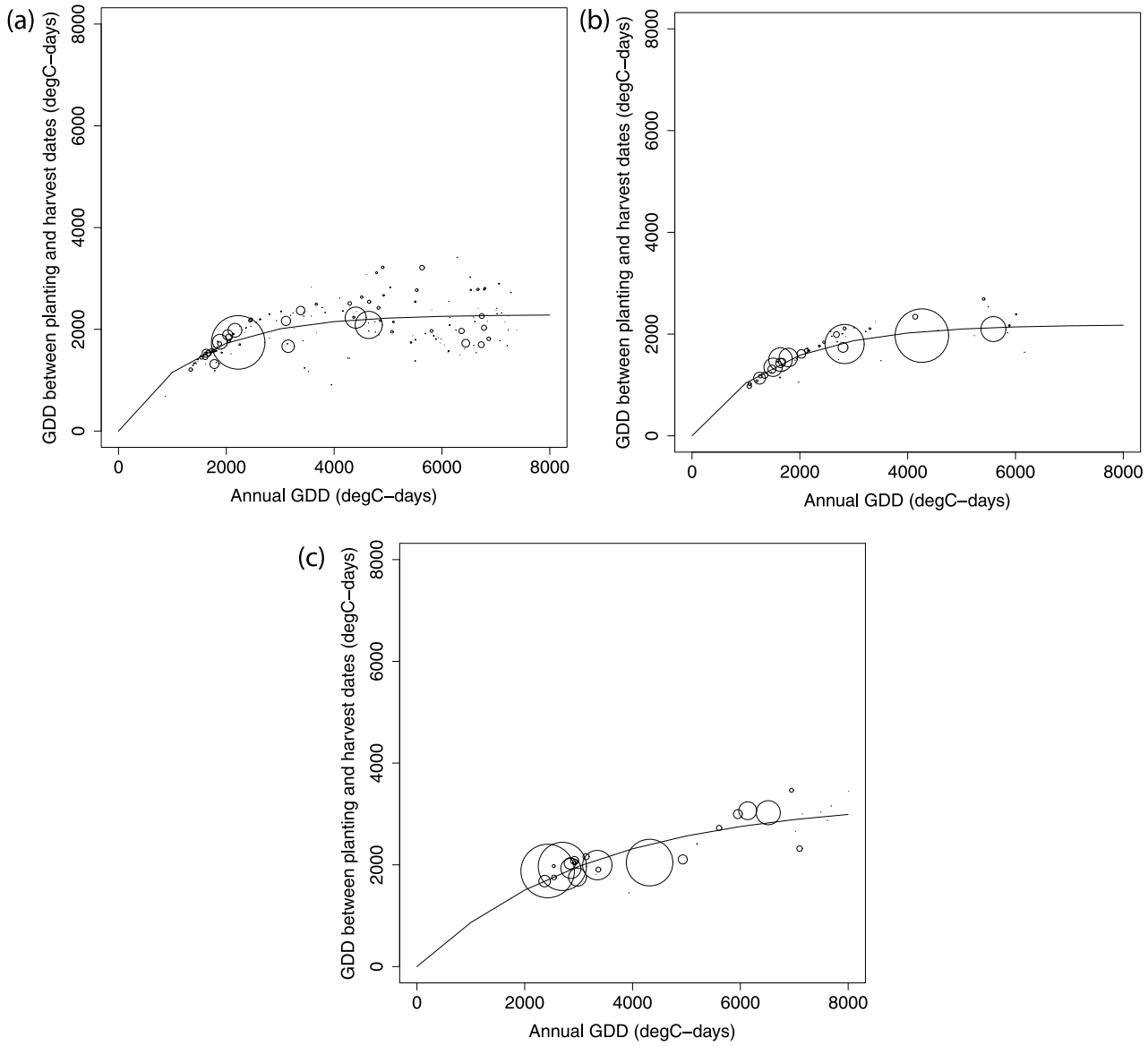

Figure 4. Scatterplots of growing degree day (GDD) accumulation between planting and harvesting dates versus annual GDD for (a) maize, (b) soybean, and (c) spring wheat. Areas of circles represent crop-harvested area.

threshold, and N is the total number of days, e.g., 365 for annual GDD calculation. Different crops have different minimum and maximum temperature thresholds for thermal accumulation. Table 2 gives specific values of T_b and $T_{\max}$.

[30] As in Agro-IBIS [*Kucharik and Brye*, 2003], we hypothesized that crop total GDD requirement is related to annual GDD. Farmers select cultivars that are adapted to the local climate: cultivars grown in colder climates have smaller GDD requirements than those grown in warmer climates. Thus, simulating harvesting decisions in the model is comparable to simulating the choice of crop cultivars as a function of the length of the growing season. Using the crop calendar data set, we calculated total GDD requirement for each crop by accumulating GDD between planting and harvesting dates. Finally, we examined the relationship between total crop GDD requirements and annual GDD, and derived simple functions from nonlinear regressions (Figure 4). We also determined a minimum GDD requirement, corresponding to the minimum average GDD between planting and harvesting dates in the data (Table 2).

2.6. Dynamic Carbon Allocation and Turnover

[31] Carbon assimilated via equation 1 is allocated to four vegetation pools: leaves, stem, roots, and storage organs. We used a descriptive allometry presented by *Penning de Vries et al.* [1989] to specify dynamic allocation and turnover fractions for each of those organs (Figure 5):

$$\frac{dC_x}{dt} = \alpha_x \mathcal{P} - \beta_x C_x \tag{9}$$

C_x is the carbon content in organs x, i.e., leaves, stem, roots, and storage organs; $\mathcal{P}$ is the daily biomass produced

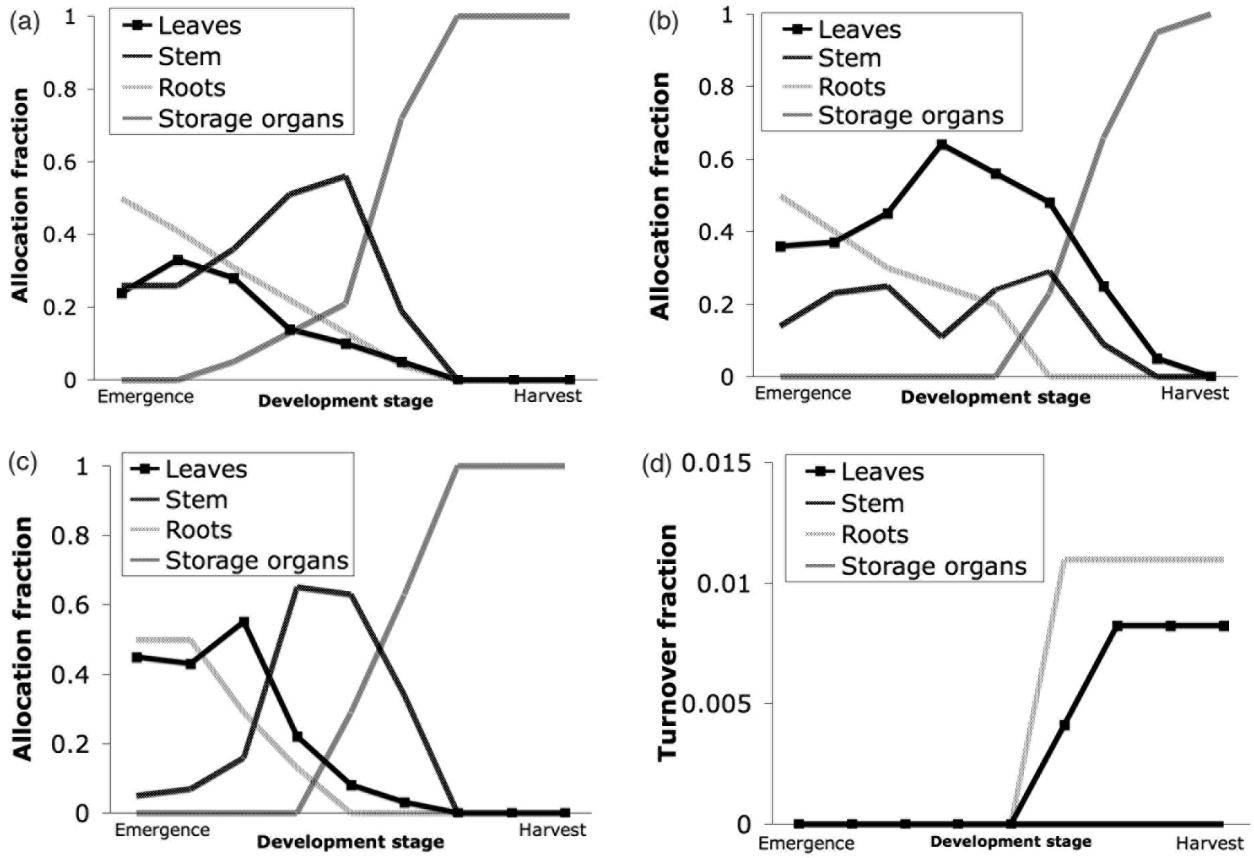

Figure 5. Dynamic carbon allocation during the growing period for (a) maize, (b) soybean, and (c) spring wheat, and (d) carbon turnover for all crops. The four different pools consist of leaves, stem, roots, and storage organs. Carbon allocation begins at emergence and ends at harvest. Carbon turnover rates for storage organs and stem remain equal to zero.

(equation (1)); and α_x and β_x are the allocation and turnover fractions, respectively (Figure 5).

[32] Allocation and turnover fractions vary with crop development, which is determined by thermal accumulation. The dynamic partitioning starts at emergence, with the duration between planting and emergence corresponding to a small fraction of the total crop GDD requirement (see Table 2 for numerical values), and ends at harvest (section 2.5.2).

[33] Crop yield (Y_e), calculated in term of fresh matter, is proportional to the amount of dry biomass accumulated in the storage organs at harvesting date (C_{so}):

$$Y_e = \frac{\mathrm{EF}}{0.45 \times \mathrm{DF}} \times C_{so}(\mathrm{t\ Ha^{-1}}) \tag{10}$$

where EF represents the economic fraction of the storage organs [*Penning de Vries et al.*, 1989], DF is the dry fraction of the economic yield to convert weight of dry matter to weight of fresh matter (Table 2), and 0.45 is the mass of carbon contained in one unit of dry matter [*Monfreda et al.*, 2008].

2.7. Simulated Cropland Extent

[34] PEGASUS simulates potential cropland area according to minimum temperature and soil moisture (ratio of precipitation to PET) thresholds and a minimum annual GDD requirement. As a consequence, PEGASUS allows crop production in some places that do not actually grow the corresponding crop type today. However, PEGASUS appears more restrictive than the actual crop-harvested area data in the northern boundaries of the high-latitude Northern Hemisphere, where minimum temperature requirement to plant and/or minimum GDD requirement to harvest is not met. Yet the discrepancy comprises a negligible fraction of the total crop-harvested area.

[35] Total cultivated area in present-day simulations (section 4.2) is the intersection of simulated and actual cropland extent for each crop. In addition, due to a lack of global data on growing areas of spring versus winter wheat, the total harvested area shown for the present-day spring wheat simulation is the intersection between actual wheat harvested area and the spring wheat crop calendar data set [*Sacks et al.*, 2010]. This excludes regions where most wheat grown is winter wheat, as well as regions where we are unsure whether spring or winter varieties dominate. For comparison, sensitivity simulations presented in section 5 include potential cultivable areas as simulated by PEGASUS.

3. Model Calibration

[36] Values of model parameters presented in Table 2 were chosen based on values commonly found in the literature. In addition, we performed a sensitivity analysis to

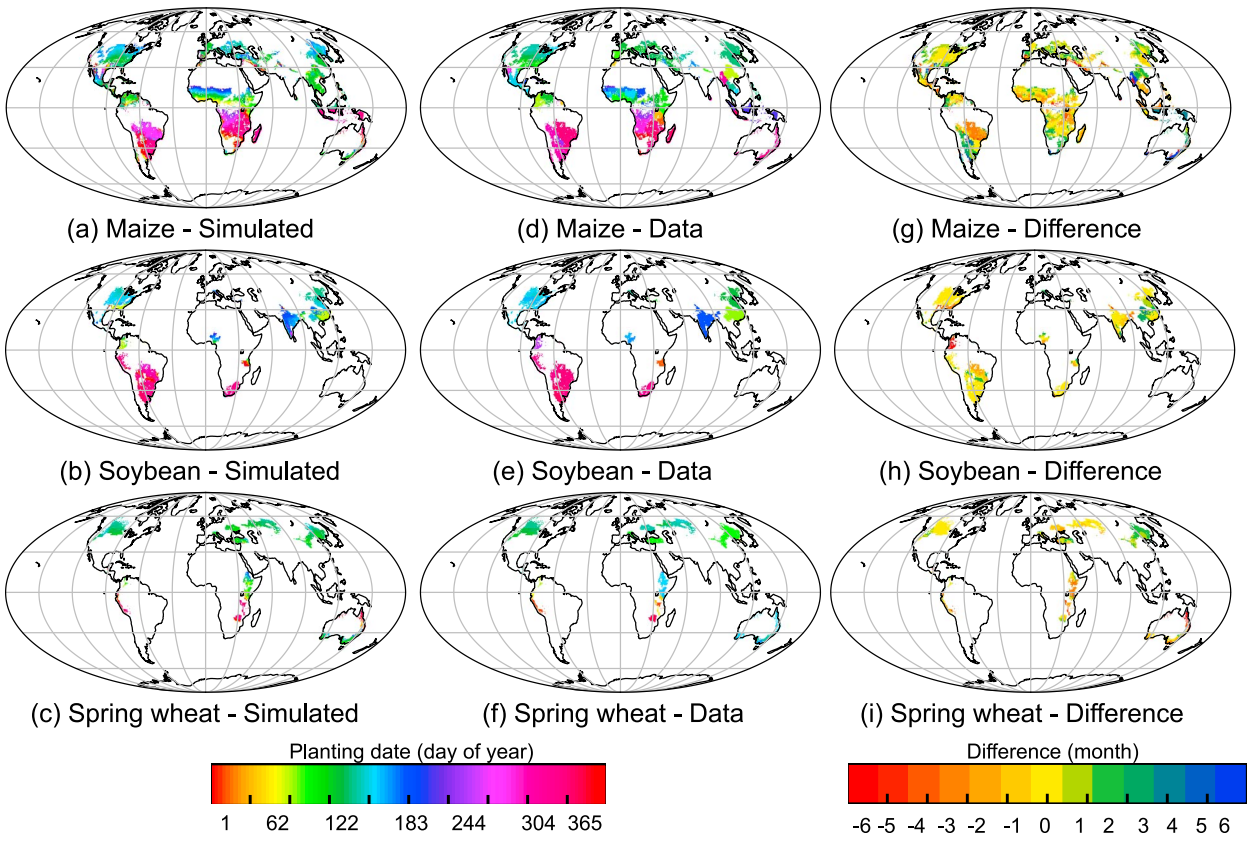

Figure 6. (a–c) Global planting dates simulated by PEGASUS and (d–f) corresponding planting date observations [*Sacks et al.*, 2010] for each crop. (g–i) The difference in months between simulated and observed planting dates.

identify which parameters had the greatest effect on simulated yields, and found the light use efficiency coefficient ε (equation (1)) to be the most important parameter.

[37] The model was calibrated against the spatial crop yield data (M3 crops data [*Monfreda et al.*, 2008]) by tuning this one variable ε. The model was run for a wide range of ε values. The calibration procedure entailed selecting the optimum ε value for each crop in two steps. First, we selected those ε values for which the systematic component of the weighted root-mean-square error (RMSE) was smaller than the unsystematic part. Then, from within these ε values, we picked the one with the highest weighted index of agreement (d) [*Willmott et al.*, 1985]. The index of agreement (d) is a standardized measure of the RMSE, and evaluates discrepancies between model prediction and observation according to the mean value of the observation. Again, the weighting is based on maps of actual crop-harvested areas [*Monfreda et al.*, 2008].

[38] The resulting values of ε expressed in mol C m^{-2} s^{-1} APAR are 0.033 for maize, 0.027 for spring wheat, and 0.011 for soybean. These global mean values coincide with the upper bound of the range found in the literature for wheat [0.022–0.027], but ε is slightly overestimated for maize [0.027–0.031] and underestimated for soybean [0.017–0.021] [*Andrade*, 1995; *Hay and Porter*, 2006; *Kiniry et al.*, 1989; *Lindquist et al.*, 2005]. In the latter case, the value of ε might be underestimated due to the absence of nutrient limitation in equation (1) (section 2.4).

[39] Although we used the same data set for calibration and evaluation of the model (presented in section 4.2), the calibration and evaluation drew on different aspects of this data set. The calibration modified only the global average ε values, whereas we evaluated the resulting model for its ability to match the spatial variability of the observations.

4. Simulation of Present-Day Crop Planting and Harvesting Dates and Yields

4.1. Planting and Harvesting Dates

[40] PEGASUS simulates planting and harvesting dates according to the rules summarized in section 2.5. Figures 6 and 7 present global maps of simulated dates, observed mean dates provided by the global crop calendar data set, and respective differences between the simulation and observations. However, in order to evaluate quantitatively the performance of our algorithm, we also compare the results to the range of dates from the data set. They give a more realistic evaluation criterion, especially in large countries where planting and harvesting times vary across regions due to differences in climate.

[41] Overall, the simulated planting dates match the range of dates given by the global crop calendar data set fairly well. Modeled planting dates show 74% agreement with observed ones in the case of maize, 91% in the case of soybean, and 75% in the case of spring wheat; the agreement is calculated here as the ratio of the harvested area of

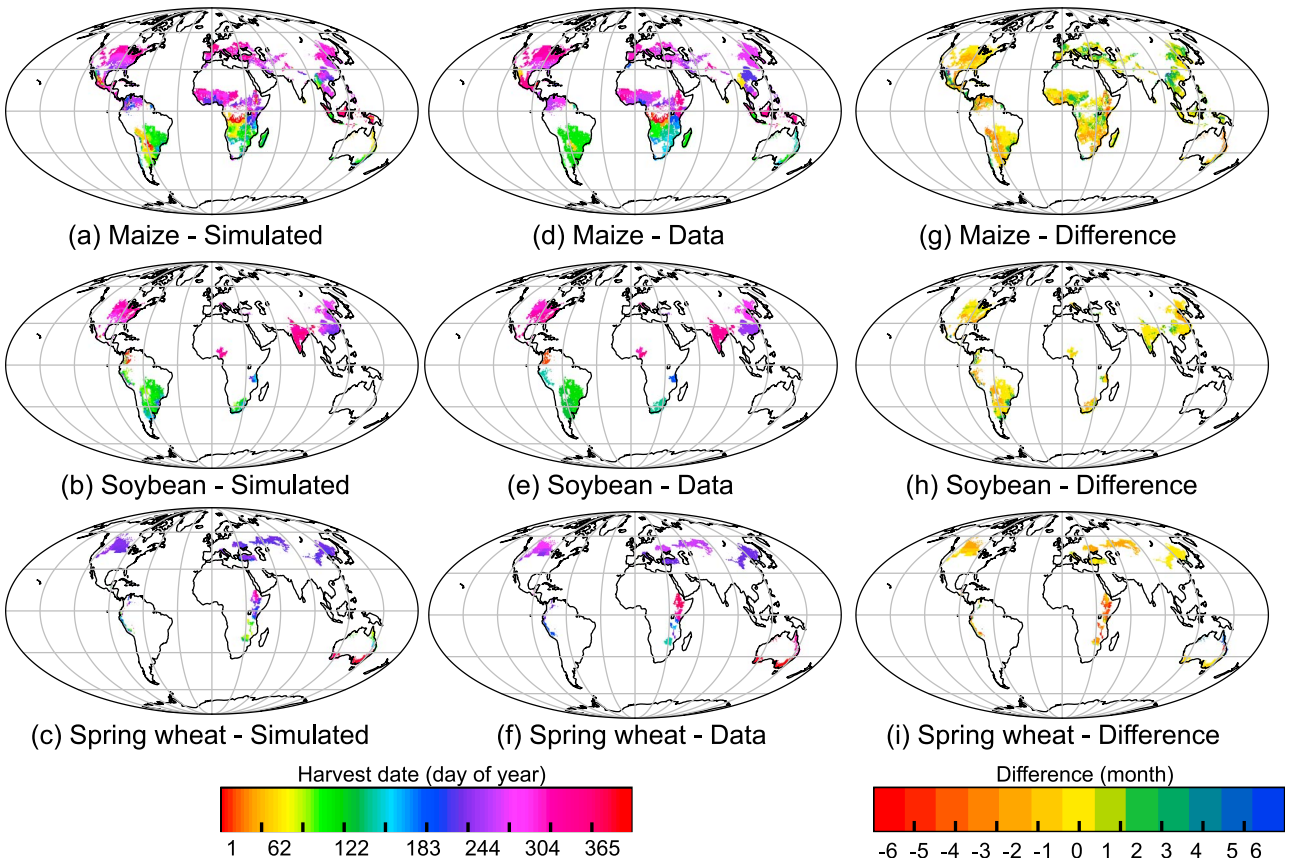

Figure 7. (a–c) Global harvesting dates simulated by PEGASUS and (d–f) corresponding harvesting date observations [*Sacks et al.*, 2010] for each crop. (g–i) The difference in months between simulated and observed harvesting dates.

all grid cells with simulated planting dates that lies within the range given by the observations to the total harvested area. For the most part, the algorithm for temperature-limited regions appears to be reasonable, whereas most of the discrepancies occur in moisture-limited regions and in non–climate-limited regions. Indeed, similar to *Stehfest et al.* [2007], most of the inconsistencies for maize occur in southeast Asian countries like Indonesia, Malaysia, and southeast China, and in southern Australia where predictions are early compared to the observations. First, simulated planting dates shift abruptly around the equator in Malaysia and Indonesia as these countries belong to non–climate-limited regions. According to our model, the planting decision is not driven by climate in those countries, and our choice of a fixed planting date is somewhat arbitrary. Secondly, our predictions in moisture-limited regions do not consider irrigation, which could also lead to differences in planting decisions, although irrigation water availability depends on the precipitation pattern as well. Similarly, soybean simulated planting dates disagree in the southeastern United States and Colombia, which are not climate limited, and in Turkey and southwest China, which are moisture-limited regions. Finally, spring wheat simulated planting dates differ mostly in Africa (i.e., Kenya, Tanzania, and Ethiopia) and northern Australia, which again are moisture-limited regions. The method presented here demonstrates that planting decisions are strongly influenced by climate factors. Additionally, it provides a set of rules to predict changes in farmers' planting decisions with climate change. However, it is important to keep in mind that socioeconomic factors also play a role in planting decisions and should be considered for realistic predictions [*Sacks et al.*, 2010].

[42] As for planting dates, the timing of harvesting decisions generally conforms to the range of harvesting dates in the data. Note that in order to assess the harvesting date algorithm independently of the planting one, we initiate the growing season using the observed planting dates. In summary, 75% of total maize harvested area is harvested within the range of harvesting dates given by the crop calendar data. The main divergences occur in non–temperature-limited regions like southern Africa, northeast Australia, southeast Asia, and central South America. Soybean and spring wheat harvesting dates are very well simulated with 92% and 99% agreement with the range of harvesting dates, but the total area simulated is smaller than for maize. Note that accuracy in modeling harvesting dates when using simulated planting dates equals 62% for maize, 91% for soybean, and 90% for spring wheat.

4.2. Crop Yields

[43] In this section, we present global crop yields simulated for present-day climate and management practices. Planting and cultivar choice decisions are simulated according to the methodology described in section 2.5. Figure 8 shows

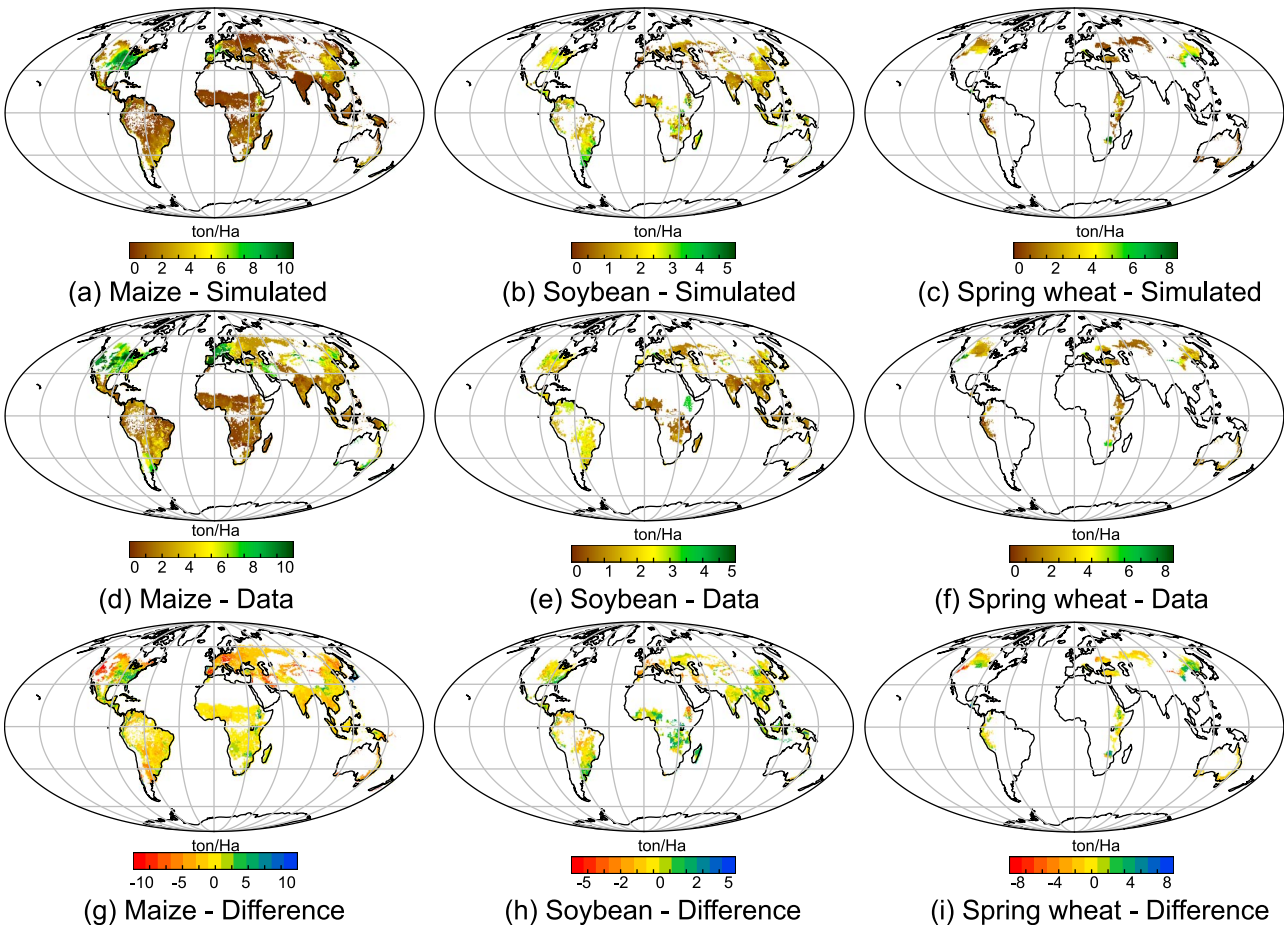

Figure 8. Global crop yields simulated by PEGASUS for (a) maize, (b) soybean, and (c) spring wheat and (d–f) corresponding crop yield observations [*Monfreda et al.*, 2008]. (g–i) The spatial differences in ton/ha between simulated and observed crop yields for each corresponding crop type.

global maps of simulated crop yields within current harvested area in comparison with actual crop yield [*Monfreda et al.*, 2008] for each of the three crops.

[44] In addition to spatial comparisons, model results are compared to national average yield derived from *Monfreda et al.* [2008]. We calculate national average yield weighted by the corresponding harvested area; we also exclude countries with total harvested area less than 1200 Ha (Figure 9). We present both weighted and unweighted coefficients of determination (R^2). Weighted R^2 is calculated based on the crop's total harvested area within each country.

[45] In the case of maize, developed countries with intensive agricultural management practices exhibit the largest yield. Highest yields are found in the United States and in western Europe, regions that apply large amounts of fertilizer. Lowest yields are found in India, Africa, and parts of Latin America. However, the model simulates lower yield than expected for eastern Europe and Russia (Figure 8). One possible explanation could be the use of manure, which is not taken into consideration in PEGASUS. Figure 9a presents a scatterplot of maize average yield for 131 countries. The R^2 is quite high when weighted by harvested areas (0.81), showing that important maize producers such as the United States, Brazil, China, Mexico, and Argentina are well simulated. However, the unweighted R^2 is only 0.37, due to discrepancies within European countries. In particular, PEGASUS underestimates yield in countries like Germany, Switzerland, Austria, the Netherlands, and Belgium.

[46] The soybean simulation includes 64 countries. While the biggest soybean producers, the United States, Brazil, Argentina, and China, are well simulated as shown in both Figures 8 and 9b, large variations exist between simulated and observed yield. In particular, yield is overestimated in African countries, whereas yield is underestimated in European countries. These differences underline a possible systematic error due to the absence of a nutrient stress factor in soybean simulations. Nevertheless, soybean harvested areas of the four top countries represent almost 90% of total soybean harvested area. As a consequence, the weighted R^2 (0.66) is reasonable, while the unweighted R^2 (0.01) remains insignificant.

[47] Finally, the global simulation of present-day yield for spring wheat is shown in Figure 8. As for the maize simulation, the global yield pattern is in agreement with global chemical fertilizer application rates. The highest yields are found in the United States, China, and Italy, while Turkey, Australia, Bolivia, and Russia exhibit lower yields. A total of 39 countries are simulated. The weighted regression analysis presented in Figure 9c results in a weighted R^2 of 0.45, while the unweighted value remains acceptable with

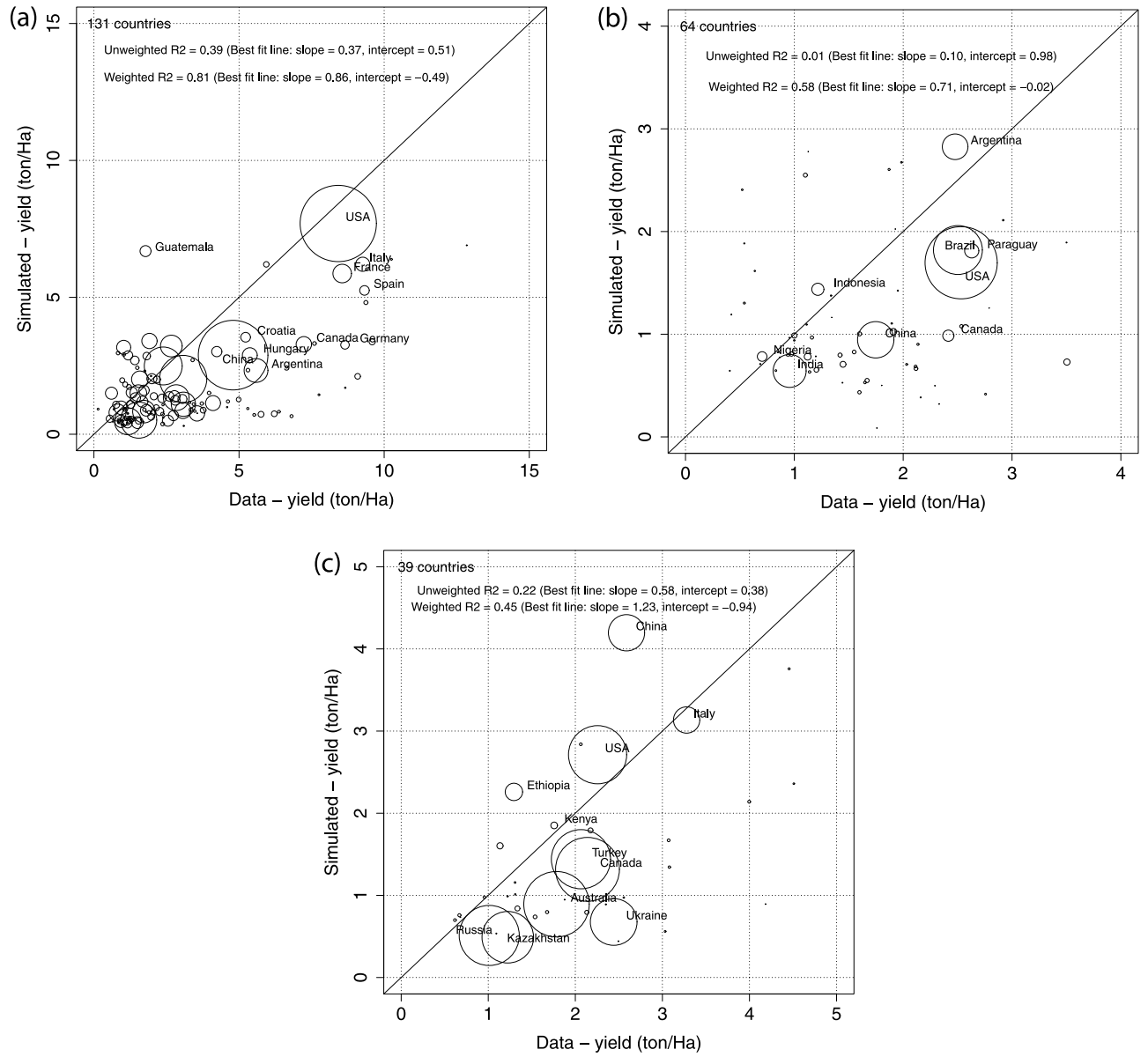

Figure 9. Comparison of simulated crop yields and corresponding observations [*Monfreda et al.*, 2008] aggregated by country for (a) maize, (b) soybean, and (c) spring wheat. Areas of circles represent crop-harvested area. We show both unweighted and weighted R^2, with the weighting based on crop-harvested area for each country, along with respective slope and intercept values of the best fit line.

0.22. Yield in China is slightly overestimated, whereas yields are mostly underestimated for a few big producers like Canada, Turkey, Kazakhstan, and Ukraine.

4.3. Comparison to Previous Studies

[48] A direct comparison with the performance of other global crop models, i.e., LPJmL and DayCent, can only be done to a limited extent. *Bondeau et al.* [2007] show a qualitative comparison between simulated and actual planting dates for temperate cereals; *Stehfest et al.* [2007] provide a comparison with the national average month of planting for maize, rice, wheat, and soybean. Further, neither of these studies evaluate the simulation of harvesting dates.

[49] Both DayCent and LPJmL provide a measure of agreement between simulated yield and national FAO data. *Bondeau et al.* [2007] evaluate simulated maize yield for 41 countries (R^2 = 0.55). The coefficients of determination for DayCent simulations of maize and soybean yields are 0.67 and 0.32, respectively (0.66 and 0.56 when weighted by crop area) [*Stehfest et al.*, 2007]. In PEGASUS, unweighted R^2 are lower, but R^2 weighted by crop areas are higher. These large differences between weighted and unweighted R^2 likely result from our approach, wherein the derived empirical equations used data weighted by present-day crop-harvested areas (sections 2.4 and 2.5). In addition, when PEGASUS was calibrated against spatial crop yield data, similar weighting by crop-harvested area was used (section 3). Consequently, PEGASUS reproduces adequately patterns of management and yield of major crop producers, but misses many small producing countries. Last, we could reduce scatter in the

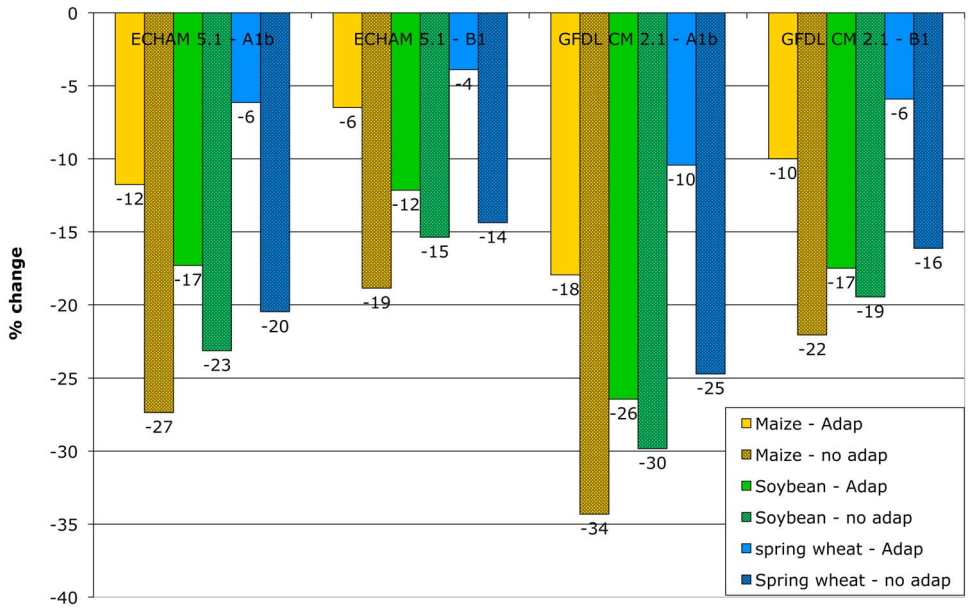

Figure 10. Estimated changes in global average crop yield by 2050 using temperature and precipitation simulations from two GCMs (ECHAM 5.1 and GFDL CM 2.1), two emissions scenarios (A1b and B1), and for the two scenarios of planting and harvesting decisions.

correlations by using spatially explicit data on fertilizer application rates (which is not available yet at the crop-specific level) rather than national average.

5. Sensitivity of Crop Yields to Variations in Temperature and Precipitation

5.1. Crop Yields

[50] In this section, we present a sensitivity analysis of the model outputs to changes in annual mean temperature and precipitation. We created monthly climatology for the 2050s using four climate change simulations from the IPCC fourth assessment report (AR4). We selected two of the better global climate models (GCMs) according to the metric developed by *Gleckler et al.* [2008]: the Geophysical Fluid Dynamics Laboratory's climate model version 2.1 (GFDL CM 2.1) and the Max-Planck Institut für Meteorologie's climate model version 5.1 (ECHAM 5.1) for both A1b and B1 emissions scenarios. Increase in annual global average temperature ranges between 1.7 (ECHAM 5.1, B1 scenario) and 2.5 (GFDL's CM 2.1, A1b scenario) by the year 2050. For this combination of two models and two scenarios, we obtained bias-corrected climate model simulation data from *Maurer et al.* [2009].

[51] We performed two sets of simulations for each of the three crops. In the first set, we used the simulated planting and harvesting dates for present-day climate, which is equivalent to preventing farmers from adjusting those decisions to any variation in temperature and precipitation. In the second set of simulations, however, farmers adapt their planting decision and their choice of crop cultivars (as simulated through the GDD requirement for crop maturity) to the new climate.

[52] In both sets of simulations, we estimated relative changes in crop yield in regions that can potentially be cropped according to our planting algorithm. On the global average (Figure 10), spring wheat yield changes the least of the three crops, with a decrease by 14 to 25% when planting decision and choice of crop cultivars remain as for present day, and a decrease by 4 to 10% when farmers fully adapt those management practices to the new temperature and precipitation patterns. Maize experiences the larger global decrease in yield for simulations preventing adaptation in planting and harvesting decisions: 19 to 34%. Soybean yield decreases by 15 to 30% without adaptation. However, soybean experiences the larger global decrease in yield for simulations allowing adaptation: 12 to 26%, while maize yield decreases by 6 to 18%. Overall, adapting planting date and cultivar choice show a stronger impact in the case of maize and spring wheat, resulting in an average reduction in global crop yield losses by 18 and 12%, respectively, whereas it shows a lesser effect in the case of soybean with an average reduction in global crop yield losses of only 7%.

[53] Figures 11, 12, and 13 display a spatial comparison of the relative change in simulated crop yield for maize, soybean, and spring wheat, respectively. Figures 11a–11h, 12a–12h, and 13a–13h present the change in crop yield simulated for each of the four different future climate simulations and the two adaptation scenarios relative to crop yield simulated using present-day climatology. In addition, Figures 11i–11l, 12i–12l, and 13i–13l present the corresponding relative change in yield resulting from adapting planting dates and crop cultivars compared to simulations without adaptation. In simulations using present-day planting dates and crop cultivars, there is a general decrease in crop yields across the globe. However, acclimating planting decisions and cultivar choices would increase yield in the high northern latitudes, due to an increase in the length of the growing season. In contrast, adapting planting dates to changes in precipitation does not present a strong impact on crop yields in tropical regions, which are also affected by heat stress as temperature increases simultaneously. This points out that

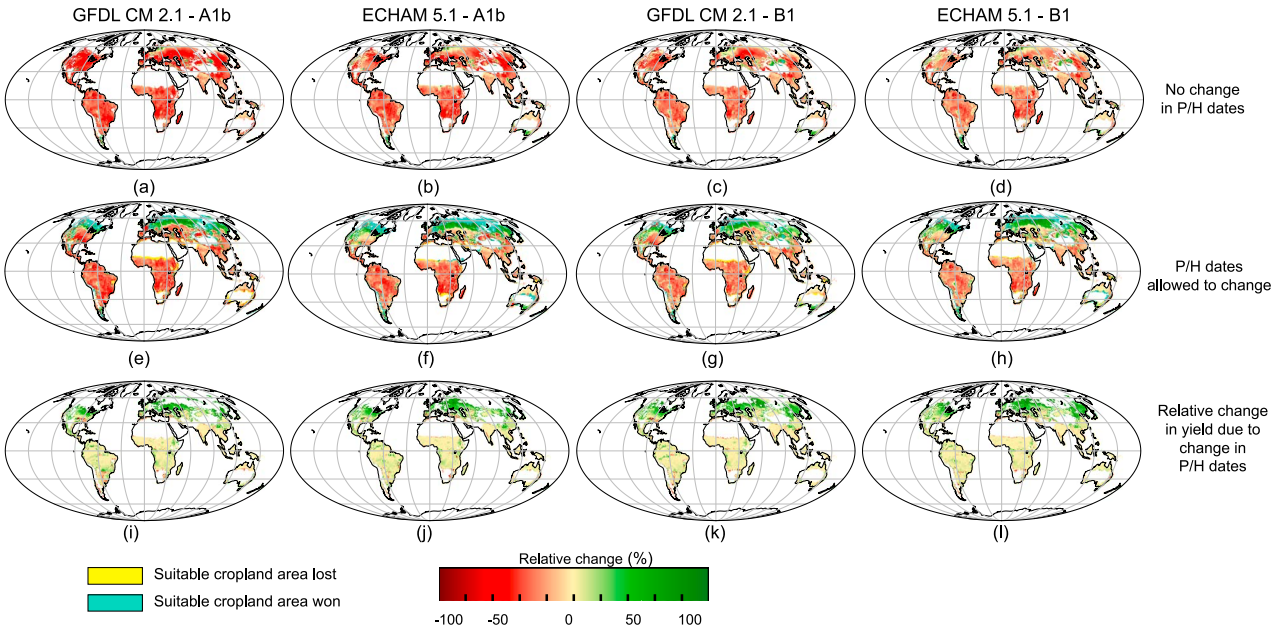

Figure 11. Estimated change (%) in maize yield by 2050, relative to the control simulation, with four different future climate simulations (a–d) for present-day planting (P) and harvesting (H) dates and (e–h) for planting and harvesting dates adapted to higher temperature. (i–l) The relative difference (%) between Figures 11a–11d and the corresponding Figures 11e–11h. White areas indicate unsuitable regions for growing crops.

the yield calculation is particularly sensitive to variations in the length and the timing of the growing season.

[54] In the case of maize (Figure 11), adaptation of planting dates and crop cultivars to the new climate results in yield increases in temperature-limited regions such as Canada, Russia, central Europe and the United Kingdom. In contrast, yield decreases despite these adaptations in western Europe, eastern and central US, northern part of Australia,

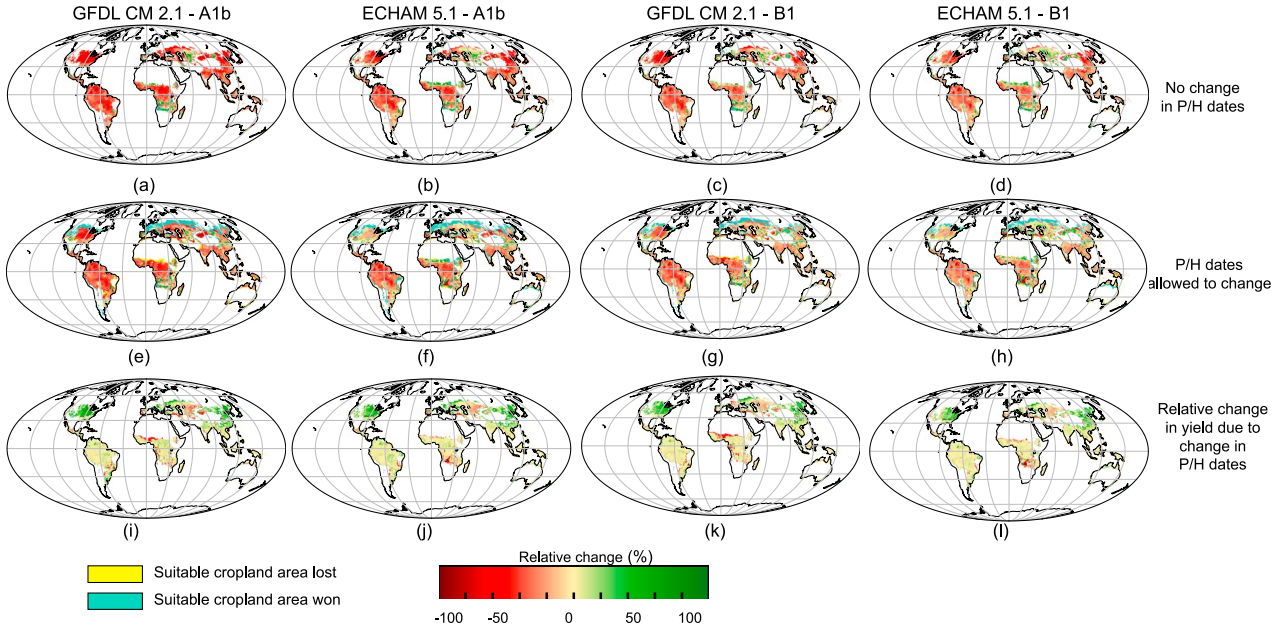

Figure 12. Estimated change (%) in soybean yield by 2050, relative to the control simulation, with four different future climate simulations (a–d) for present-day planting (P) and harvesting (H) dates and (e–h) for planting and harvesting dates adapted to higher temperature. (i–l) The relative difference (%) between Figures 12a–12d and the corresponding Figures 12e–12h. White areas correspond to unsuitable regions for growing crops.

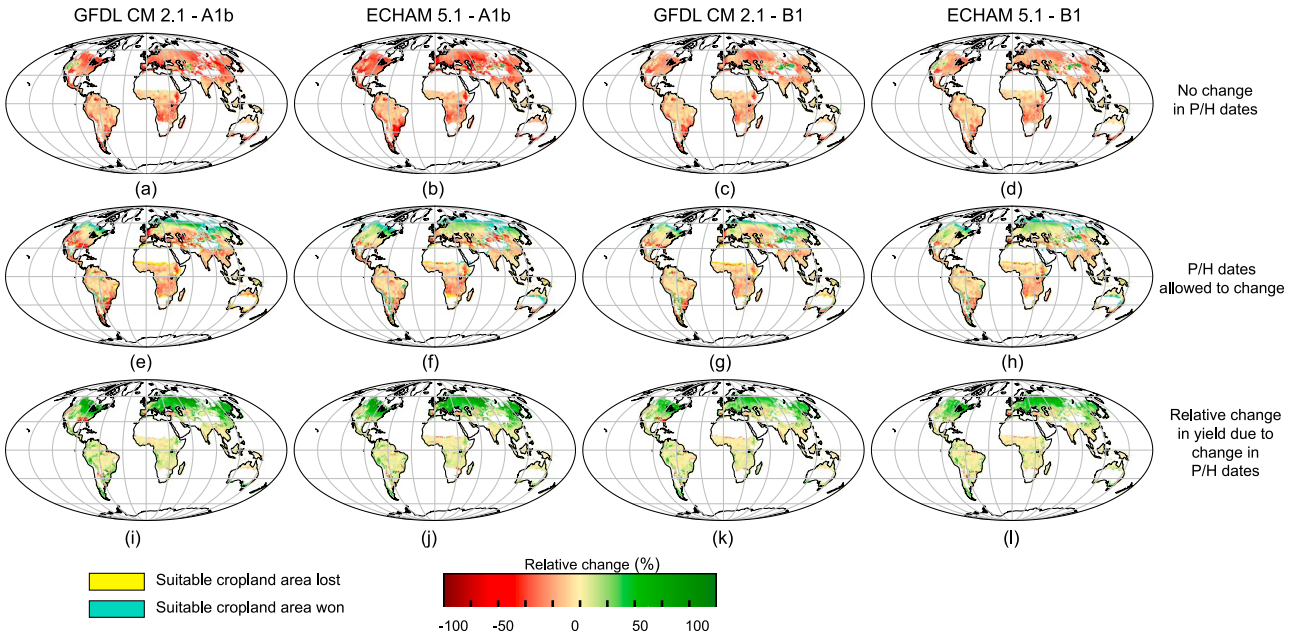

Figure 13. Estimated change (%) in spring wheat yield by 2050, relative to the control simulation, with four different future climate simulations (a–d) for present-day planting (P) and harvesting dates (H) and (e–h) for planting and harvesting dates adapted to higher temperature. (i–l) The relative difference (%) between Figures 13a–13d and the corresponding Figures 13e–13h. White areas correspond to unsuitable regions for growing crops.

southeast Asia, and all of India, Africa, and Latin America. Nevertheless, adapting planting and harvesting decisions reduces crop yield losses in the US, Europe, and East Asia.

[55] Relative changes in spring wheat yields show very similar patterns as for maize simulations (Figure 13). However, losses are less substantial in the US and the western European countries. Furthermore, the expansion of suitable cropland area is smaller than for maize.

[56] Finally, adapting planting dates and crop cultivars expands the suitable area for soybean production in some parts of Europe and northeast Asia. Crop yield losses are minimized in the eastern US and East Asia (Figure 12). However, adapting those decisions in some places with significant reductions in precipitation, mainly in Africa, western Spain, and Cuba, shows a negative effect on yield. Those anomalies highlight potential limitations of planting changes in moisture-limited regions.

5.2. Comparison to Previous Studies

[57] In this section, we compare our simple sensitivity analysis to previous studies of the effects of climate change on global crop yield. *Rosenzweig and Parry* [1994] estimated that global cereal production would decrease by 11 to 20% when considering only the direct effect of climate change, and by 1 to 8% when including the CO_2 fertilization effect (global mean temperature increases by ~4 to 5, global precipitation increases by ~8 to 15%, and CO_2 concentration increases by ~600 to 640 p.p.m. in their scenarios).

[58] *Leemans and Solomon* [1993], who performed a basic analysis of the effect of changes in temperature on global crop yield, found a decrease in global potential rain-fed crop yields of roughly 15% assuming no change in suitable cultivated area. However, they took into account rain-fed agriculture only, while we examined both irrigated and rain-fed agriculture. Considering only rain-fed cropland area, we also observe a global decrease in yield of 14% for maize, 16% for soybean, and 18% for spring wheat on average when adapting planting dates and crop cultivars.

[59] More recently, *Nelson et al.* [2009] estimated changes in yield ranging from −2 to −8.7% for irrigated maize (from 1.4 to −5.7% for rain-fed maize) and from −4.9 to −34.3% for irrigated wheat (from −1.4 to 3.1% for rain-fed wheat). In our study, global relative changes in yield similarly range between −1% and 6% for irrigated maize (according to present-day maize irrigated area) for the adaptation scenarios. However, relative changes in yield for irrigated spring wheat and irrigated soybean areas are larger than for rain-fed areas, ranging from −12 to −24% for spring wheat and from −19% to −38% for soybean. But irrigation in our analysis is simplistic as it does not include any information on water availability or any information on potential increase in irrigated cropland area.

6. Conclusion

[60] This study presents a simple modeling approach to quantify global crop yields and the role of agricultural management practices on crop productivity. We demonstrate the importance of planting and cultivar choices on crop yields in relation to variations in temperature. We developed simple rules to derive planting and cultivar choice decisions according to variations in temperature, precipitation, and potential evapotranspiration. For each crop considered in this study, more than 60% of the total harvested area is planted and harvested within the range of observed dates. Nonetheless, the planting date algorithm works better in

temperature-limited regions, and not as well in moisture-limited regions. PEGASUS's performance in simulating crop yields is comparable to that of other global crop models.

[61] In addition, we evaluate the implication of changes in monthly mean temperature and precipitation on yields along with the effect of adapting planting dates and cultivar choices to these new climatic conditions. We found that these management practices could play a crucial role in mitigating the negative impact of climate change on world food production, as they could avoid predicted global yield losses by 18% for maize, 12% for spring wheat, and 7% for soybean.

[62] PEGASUS relies on few parameters, which allows its broad and straightforward application. However, several improvements remain necessary. First of all, simulation of nutrient limitation could be improved by including the effects of manure in the model, and by reconsidering the effects of nutrients on soybean yield. We could also improve upon the simple empirical approach used here to consider nutrient influence. In addition, improvements should be made with respect to the influence of soil water on nutrient stress. Second, it is desirable to incorporate other crops into the model, such as winter wheat and rice, and other non-cereal crops, in order to comprehensively assess world food production. Third, improvements in the simulation of water availability for irrigation are mandatory for realistic climate change impact assessments. Finally, additional factors that should be considered, but whose influences are still being debated, include the physiological effect of increasing atmospheric CO_2 on biomass production and on crop water use, as well as the impact of future pest and disease behaviors on agricultural systems [*Long*, 2006; *Tubiello et al.*, 2007].

[63] **Acknowledgments.** We would like to thank Jonathan Foley for his contribution to the early stages of model development. We are also grateful to Nigel Roulet and Jianghua Wu for providing helpful guidance regarding the model calibration and evaluation, Deepak Ray for providing us with the GCM's data in a suitable format, and Amy Kimbal and Pedram Rowhani for their constructive comments on an initial draft of this manuscript. Finally, the helpful comments of Eric Sundquist and two anonymous reviewers significantly improved this manuscript. This work was accomplished through financial support to Navin Ramankutty from the U.S. Environmental Protection Agency (subcontract from Purdue University) and from the Canadian Natural Science and Engineering Research Council (NSERC) awards from the Global Environmental and Climate Change Center (GEC3) to Delphine Deryng, and an NSF Graduate Research Fellowship supporting William Sacks.

References

Andrade, F. H. (1995), Analysis of growth and yield of maize, sunflower and soybean grown at Balcarce, Argentina, *Field Crops Res.*, *41*, 1–12.

Batjes, N. H. (2006), Isric-wise derived soil properties on a 5 by 5 arc-minutes global grid, *Rep. 2006/02*, ISRIC-World Soil Inf., Wageningen, Netherlands. (Available at http://www.isric.org.)

Bondeau, A., et al. (2007), Modelling the role of agriculture in the 20th century global terrestrial carbon balance, *Global Change Biol.*, *13*, 679–706, doi:10.1111/j.1365-2486.2006.01305.x.

Campbell, G. S., and J. M. Norman (2000), *An Introduction to Environmental Biophysics*, 2nd ed., Springer, Berlin.

Cassman, K. G. (1999), Ecological intensification of cereal production systems: Yield potential, soil quality, and precision agriculture, *Proc. Natl. Acad. Sci.*, *96*, 5952–5959, doi:10.1073/pnas.96.11.5952.

de Noblet-Ducoudré, N., S. Gervois, P. Ciais, N. Viovy, N. Brisson, B. Seguin, and A. Perrier (2004), Coupling the Soil-Vegetation-Atmosphere-Transfer Scheme ORCHIDEE to the agronomy model STICS to study the influence of croplands on the European carbon and water budgets, *Agronomie*, *24*(6–7), 397–407, doi:10.1051/agro:2004038.

Fischer, G., M. Shah, and H. V. Velthuizen (2002a), Climate change and agricultural vulnerability, report, Int. Inst. for Appl. Syst. Anal., Laxenburg, Austria.

Fischer, G., M. Shah, H. Velthuizen, and F. Nachtergaele (2002b), Global agro-ecological assessment for agriculture in the 21st century, report, Int. Inst. for Appl. Syst. Anal., Laxenburg, Austria.

Foley, J. A. (1994), Net primary productivity in the terrestrial biosphere: The application of a global model, *J. Geophys. Res.*, *99*(D10), 20,773–20,783.

Foley, J. A., C. Monfreda, N. Ramankutty, and D. Zaks (2007), Our share of the planetary pie, *Proc. Natl. Acad. Sci.*, *104*(31), 12,585–12,586, doi:10.1073pnas.0705190104.

Food and Agriculture Organization (FAO) (1978), Report on the agro-ecological zones project, vol. 1, Methodology and results for africa, of the United Nations, Rome, Italy.

Food and Agriculture Organization (FAO) (2009), FAOSTAT, Statistical Databases, http://faostat.fao.org/default.aspx, United Nations, Rome, Italy.

Gerten, D., S. Schaphoff, U. Haberlandt, W. Lucht, and S. Sitch (2004), Terrestrial vegetation and water balance–hydrological evaluation of a dynamic global vegetation model, *J. Hydrol.*, *286*(1–4), 249–270, doi:10.1016/j.jhydrol.2003.09.029.

Gervois, S., N. de Noblet-Ducoudré, N. Viovy, P. Ciais, N. Brisson, B. Seguin, and A. Perrier (2004), Including croplands in a global biosphere model: Methodology and evaluation at specific sites, *Earth Interact.*, *8*, 1–25.

Gervois, S., P. Ciais, N. de Noblet-Ducoudré, N. Brisson, N. Vuichard, and N. Viovy (2008), Carbon and water balance of European croplands throughout the 20th century, *Global Biogeochem. Cycles*, *22*, GB2022, doi:10.1029/2007GB003018.

Gleckler, P. J., K. E. Taylor, and C. Doutriaux (2008), Performance metrics for climate models, *J. Geophys. Res.*, *113*, D06104, doi:10.1029/2007JD008972.

Harris, J. M., and S. Kennedy (1999), Carrying capacity in agriculture: Global and regional issues, *Ecol. Econ.*, *29*(3), 443–461.

Haxeltine, A., and I. Prentice (1996), A general model for the light-use efficiency of primary production, *Funct. Ecol.*, *10*, 551–561.

Hay, R. K. M., and J. R. Porter (2006), *The Physiology of Crop Yield*, 2nd ed., Wiley-Blackwell, Cambridge, U. K.

Howden, S. M., J.-F. Soussana, F. N. Tubiello, N. Chhetri, M. Dunlop, and H. Meinke (2007), Adapting agriculture to climate change, *Proc. Natl. Acad. Sci.*, *104*(50), 19,691–19,696, doi:10.1073pnas.0701890104.

International Fertilizer Industry Association (2002), *Fertilizer Use by Crop*, 5th ed., Food and Agric. Org., United Nations, Rome, Italy.

Keyzer, M., M. Merbis, and F. Pavel (2002), Can we feed the animals? Origins and implications of rising meat demand, paper presented at 2002 International Congress, Eur. Assoc. of Agric. Econ., Zaragoza, Spain, 28–31 Aug.

Kiniry, J. R., C. A. Jones, J. C. O'Toole, R. Blanchet, M. Cabelguenne, and D. A. Spanel (1989), Radiation-use efficiency in biomass accumulation prior to grain-filling for five grain-crop species, *Field Crops Res.*, *20*, 1–14.

Kucharik, C. J. (2008), Contribution of planting date trends to increased maize yields in the central United States, *Agron. J.*, *100*(2), 1–9, doi:10.2134/agronj2007.0145.

Kucharik, C. J., and K. R. Brye (2003), Integrated BIosphere Simulator (IBIS) and nitrate loss predictions for Wisconsin maize receiving varied amounts of nitrogen fertilizer, *J. Environ. Qual.*, *32*, 247–268.

Leemans, R., and A. Solomon (1993), Modeling the potential change in yield and distribution of the earth's crops under a warmed climate, *Clim. Res.*, *3*, 79–96.

Licker, R., M. Johnston, C. Barford, J. Foley, C. Monfreda, and N. Ramankutty (2010), Mind the gap: How do climate and agricultural management explain the 'yield gap' of croplands around the world?, *Global Ecol. Biogeogr.*, *19*(6), 769–782.

Lindquist, J., T. Arkebauer, D. T. Walters, K. G. Cassman, and A. Dobermann (2005), Maize radiation use efficiency under optimal growth conditions, *Agron. J.*, *97*, 72–78.

Lobell, D. B., and G. P. Asner (2003), Climate and management contributions to recent trends in U.S. agricultural yields, *Science*, *299*(5609), 1032, doi:10.1126/science.1077838.

Lobell, D. B., and C. B. Field (2007), Global scale climate-crop yield relationships and the impacts of recent warming, *Environ. Res. Lett.*, *2*, 1–7, doi:10.1088/1748-9326/2/1/014002.

Lobell, D. B., M. B. Burke, C. Tebaldi, M. D. Mastrandrea, W. Falcon, and R. Naylor (2008), Prioritizing climate change adaptation needs for food security in 2030, *Science*, *319*(5863), 607–610, doi:10.1126/science.1152339.

Long, S. P. (2006), Food for thought: Lower-than-expected crop yield stimulation with rising CO2 concentrations, *Science*, *312*(5782), 1918–1921, doi:10.1126/science.1114722.

Lotze-Campen, H., C. Müller, A. Bondeau, S. Rost, A. Popp, and W. Lucht (2008), Global food demand, productivity growth, and the scarcity of land and water resources: A spatially explicit mathematical programming approach, *Agric. Econ.*, *39*(3), 325–338, doi:10.1111/j.1574-0862.2008.00336.x.

Lutz, W., W. Sanderson, and S. Scherbov (2001), The end of world population growth, *Nature*, *412*, 543–545, doi:10.1038/35087589.

Maurer, E. P., J. C. Adam, and A. W. Wood (2009), Climate model based consensus on the hydrologic impacts of climate change to the rio lempa basin of central america, *Hydrol. Earth Syst. Sci.*, *13*(2), 183–194, doi:10.5194/hess-13-183-2009.

Monfreda, C., N. Ramankutty, and J. A. Foley (2008), Farming the planet: 2. Geographic distribution of crop areas, yields, physiological types, and net primary production in the year 2000, *Global Biogeochem. Cycles*, *22*, GB1022, doi:10.1029/2007GB002947.

Nelson, G. C., et al. (2009), *Climate Change: Impact on Agriculture and Costs of Adaptation*, Int. Food Policy Res. Inst., Washington, D. C.

New, M., D. Lister, M. Hulme, and I. Makin (2002), A high-resolution data set of surface climate over global land areas, *Clim. Res.*, *21*, 1–25.

Osborne, T. M., D. M. Lawrence, A. J. Challinor, J. M. Slingo, and T. R. Wheeler (2007), Development and assessment of a coupled crop–climate model, *Global Change Biol.*, *13*, 169–183, doi:10.1111/gcb.2007.13.issue-1.

Parry, M., C. Rosenzweig, A. Iglesias, G. Fischeer, and M. Livermore (1999), Climate change and world food security: A new assessment, *Global Environ. Change*, *9*, 551–567.

Parry, M., C. Rosenzweig, and M. Livermore (2005), Climate change, global food supply and risk of hunger, *Philos. Trans. R. Soc. London, Ser. B*, *360*, 2125–2138, doi:10.1098/rstb.2005.1751.

Penning de Vries, F. W. T., D. M. Jansen, H. F. M. ten Berge, and A. Bakema (1989), *Simulation of Ecophysiological Processes of Growth in Several Annual Crops*, Pudoc, Wageningen, Netherlands.

Portmann, F. T., S. Siebert, and P. Döll (2010), MIRCA2000—Global monthly irrigated and rainfed crop areas around the year 2000: A new high-resolution data set for agricultural and hydrological modeling, *Global Biogeochem. Cycles*, *24*, GB1011, doi:10.1029/2008GB003435.

Postel, S. L. (1998), Water for food production: Will there be enough in 2025?, *Bioscience*, *48*(8), 629–637.

Ramankutty, N., J. A. Foley, J. Norman, and K. McSweeney (2002), The global distribution of cultivable lands: Current patterns and sensitivity to possible climate change, *Global Ecol. Biogeogr.*, *11*, 377–392.

Rosenzweig, C., and M. Parry (1994), Potential impact of climate change on world food supply, *Nature*, *367*, 133–138.

Sacks, W. J., D. Deryng, J. A. Foley, and N. Ramankutty (2010), Crop planting dates: An analysis of global patterns, *Global Ecol. Biogeogr.*, *19*(5), 607–620.

Salvagiotti, F., K. Cassman, J. Specht, D. Walters, A. Weiss, and A. Dobermann (2008), Nitrogen uptake, fixation and response to fertilizer N in soybeans: A review, *Field Crops Res.*, *108*, 1–13.

Schlenker, W., and M. J. Roberts (2009), Nonlinear temperature effects indicate severe damages to U.S. crop yields under climate change, *Proc. Natl. Acad. Sci.*, *106*(37), 15,594–15,598, doi:10.1073/pnas.0906865106.

Scholze, M., A. Bondeau, F. Ewert, C. Kucharik, J. Priess, and P. Smith (2005), Advances in large-scale crop modeling, *Eos Trans. AGU*, *86*(26), 245, doi:10.1029/2005EO260002.

Sharpley, A., and J. Williams (1990), *EPIC, Erosion/Productivity Impact Calculator*, Agric. Res. Serv., U.S. Dep. of Agric., Washington, D. C.

Stehfest, E., M. Heistermann, J. Priess, D. Ojima, and J. M. Alcamo (2007), Simulation of global crop production with the ecosystem model DayCent, *Ecol. Econ.*, *209*, 203–219, doi:10.1016/j.ecolmodel.2007.06.028.

Tilman, D., J. Fargione, and B. Wolff (2001), Forecasting agriculturally driven global environmental change, *Science*, *292*(5515), 281–284, doi:10.1126/science.1057544.

Tilman, D., K. G. Cassman, P. Matson, R. Naylor, and S. Polasky (2002), Agricultural sustainability and intensive production practices, *Nature*, *418*, 671–677, doi:doi:10.1038/nature01014.

Tubiello, F. N., J.-F. Soussana, and S. M. Howden (2007), Crop and pasture response to climate change, *Proc. Natl. Acad. Sci.*, *104*(50), 19,686–19,690, doi:10.1073pnas.0701728104.

Von Braun, J. (2007), *The World Food Situation. New Driving Forces and Required Actions*, Int. Food Policy Res. Inst., Washington, D. C.

Willmott, C. J., S. G. Ackleson, R. E. Davis, J. J. Feddema, K. M. Klink, D. R. Legates, J. O'Donell, and C. M. Rew (1985), Statistics for the evaluation and comparison of models, *J. Geophys. Res.*, *90*(C5), 8995–9005.

C. C. Barford and W. J. Sacks, SAGE, 1710 University Ave., Madison, WI 53726, USA.

D. Deryng, Tyndall Centre, School of Environmental Sciences, University of East Anglia, Norwich, NR4 7TJ, UK. (d.deryng@uea.ac.uk)

N. Ramankutty, Department of Geography, McGill University, 805 Sherbrooke St. W., Montreal QC H3A 2K6, Canada.